Journal of Spacecraft and Rockets, Vol. 57, No. 5, 2020, pp. 1098–1102. doi: http://doi.org/10.2514/1.A34709

Role of solar irradiance fluctuations on optimal solar sail trajectories

Andrea Caruso,* Lorenzo Niccolai,† Alessandro A. Quarta,‡ and Giovanni Mengali§

Department of Civil and Industrial Engineering, University of Pisa, I-56122 Pisa, Italy

Nomenclature

A	=	sail surface, m^2
$\boldsymbol{a}$	=	propulsive acceleration vector, $\mathrm{mm/s^2}$
a_c	=	characteristic acceleration, $\mathrm{mm/s^2}$
$\{b_1, b_2, b_3\}$	=	sail force coefficients
c	=	speed of light, km/s
m	=	total spacecraft mass, kg
$\hat{\boldsymbol{n}}$	=	normal unit vector
$P_\oplus$	=	solar radiation pressure at 1 au, Pa
$\boldsymbol{r}$	=	position vector, au
r	=	Sun-spacecraft distance, au
$r_\oplus$	=	reference distance, 1 au
t	=	time, days
$\boldsymbol{v}$	=	velocity vector, km/s
$W_\oplus$	=	total solar irradiance at $r = r_\oplus$, $\mathrm{W/m^2}$
$W_\oplus^{\min}$	=	value of $W_\oplus$ during minimum solar activity, $\mathrm{W/m^2}$
δ_r	=	final position error, km
δ_v	=	final velocity error, m/s
$\mu_\odot$	=	Sun's gravitational parameter, $\mathrm{km^3/s^2}$
μ_W	=	mean value of $W_\oplus$ as a function of time, $\mathrm{W/m^2}$
σ_W	=	standard deviation of $W_\oplus$, $\mathrm{W/m^2}$

Subscripts

0	=	initial value
f	=	final value

Superscripts

$\cdot$	=	time derivative
$\wedge$	=	unit vector
$-$	=	reference value

Introduction

The analysis and optimization of a solar sail trajectory is usually conducted by assuming a constant value of the total solar irradiance (TSI) and, therefore, of the solar radiation pressure (SRP) [1, 2]. Actually, the TSI (or the SRP) is subjected to time-variations [3] caused by the well known 11-year solar cycle, and by non-negligible short-term random fluctuations [4–6]. A refined solar sail mission analysis should therefore take into account the effects of those temporal variations.

The original idea of studying the effects of TSI fluctuations on solar sail heliocentric trajectories is due to Vulpetti [7, 8], who considered the actual values of the SRP (obtained through in-situ measurements) during the simulation of an Earth-Mars transfer orbit of a solar sail-based spacecraft. However, such works are focused on medium- and high-performance solar sails only, and rely on TSI data obtained for a limited time span (about two years). More recently, Niccolai et al. [9] have studied the effects of TSI fluctuations and optical parameter uncertainties on the trajectory of a Sun-facing sail.

The aim of this work is to provide a systematic analysis for quantifying the impact of TSI fluctuations on minimum-time solar sail trajectories, in order to investigate the actual need of a control law able to counteract the environmental uncertainties, as is discussed in Refs. [10, 11] for the case of an electric solar wind sail [12]. To that end, a procedure to evaluate the effects of TSI (or SRP) fluctuations is here proposed, which consists of modelling the solar irradiance as the combination of a periodic and a stochastic term. Such a method is based on a large amount of TSI data. Some possible heliocentric mission scenarios for a high- or low-performance sail are analyzed, such as, for example, a simplified circle-to-circle orbit raising and a more realistic three-dimensional transfer towards a near-Earth asteroid.

The Note is organized as follows. First, the mathematical model used to describe the propulsive acceleration and the transfer orbit is introduced. Then, a procedure to evaluate the effects of environmental uncertainties on a solar sail-based spacecraft trajectory is proposed assuming the TSI to be modelled as a random variable with a Gaussian distribution. Finally, the proposed approach is used to analyze some exemplary mission cases, while the last section reviews the main outcomes of this work.

*Ph.D. student, andrea.caruso@ing.unipi.it (**corresponding author**).
†Research assistant, lorenzo.niccolai@ing.unipi.it.
‡Professor, a.quarta@ing.unipi.it. Associate Fellow AIAA.
§Professor, g.mengali@ing.unipi.it. Senior Member AIAA.

Effects of TSI fluctuations

Consider a solar sail-based spacecraft that performs an ephemeris-free heliocentric transfer between a given parking orbit (subscript 0) and an assigned target orbit (subscript f). Assuming a flat sail with an optical force model [2], its propulsive acceleration vector $\boldsymbol{a}$ may be written as

$$\boldsymbol{a} = \frac{W_\oplus\, A}{c\, m} \left(\frac{r_\oplus}{r}\right)^2 (\hat{\boldsymbol{n}} \cdot \hat{\boldsymbol{r}}) \left[b_1 \hat{\boldsymbol{r}} + (b_2 \hat{\boldsymbol{n}} \cdot \hat{\boldsymbol{r}} + b_3)\hat{\boldsymbol{n}}\right] \tag{1}$$

where r is the Sun-spacecraft distance (with $r_\oplus \triangleq 1\,\mathrm{au}$), c is the speed of light, $W_\oplus$ is the total solar irradiance measured at $r = r_\oplus$ (recall [2] that the SRP at $r = r_\oplus$ is $P_\oplus = W_\oplus/c$), A is the sail reflective area, m is the total spacecraft mass, $\hat{\boldsymbol{r}}$ is the Sun-spacecraft (radial) unit vector, $\hat{\boldsymbol{n}}$ is the unit vector normal to the sail plane in the direction opposite to the Sun, and $\{b_1,\, b_2,\, b_3\}$ are the force coefficients that depend on the thermo-optical properties of the sail reflective film [13]. In particular, when the sail degradation [14,15] is neglected and the reflective film does not include electrochromic material panels [16,17], the force coefficients $\{b_1,\, b_2,\, b_3\}$ take constant values, given by [2] $b_1 = 0.1728$, $b_2 = 1.6544$ and $b_3 = -0.0109$. The desired thrust vector direction [18] is obtained by varying the sail plane orientation, that is, by suitably steering the normal unit vector $\hat{\boldsymbol{n}}$. Note that the orientation of $\hat{\boldsymbol{n}}$ in an orbital (radial-tangential-normal) reference frame is described by the cone and clock angles, which are usually the two controls of a flat solar sail. The time-orientation of the normal unit vector $\hat{\boldsymbol{n}}$ or, equivalently, the time-variation of the sail cone and clock angles, is obtained by solving an optimization problem [13,19,20] in which the flight time between the parking and the target orbit is to be minimized.

The solar sail heliocentric dynamics is described by the equations

$$\dot{\boldsymbol{r}} = \boldsymbol{v} \quad , \quad \dot{\boldsymbol{v}} = -\frac{\mu_\odot}{r^3}\boldsymbol{r} + \boldsymbol{a} \tag{2}$$

where the dot symbol denotes a derivative with respect to time t, $\boldsymbol{r} = r\,\hat{\boldsymbol{r}}$ and $\boldsymbol{v}$ are the spacecraft position and velocity vector, respectively, $\mu_\odot$ is the Sun's gravitational parameter, and $\boldsymbol{a}$ is given by Eq. (1).

In a preliminary mission analysis, the spacecraft optimal transfer trajectory is designed assuming constant solar properties, which amounts to considering a fixed value of TSI in Eq. (1). In that case, once the minimum time problem is solved and the control law $\hat{\boldsymbol{n}} = \hat{\boldsymbol{n}}(t)$ is obtained from the optimization problem, the equations of motion (2) may be numerically integrated to get a reference transfer trajectory. However, because the value of TSI is not actually a constant [3], the effects of the variability of $W_\oplus$ on the reference transfer trajectory require further investigation.

Indeed, it is known that the TSI undergoes fluctuations over time, mainly due to the 11-year solar cycles [4]. Recent in-situ measurements, carried out by the SORCE spacecraft during a solar minimum activity period [5,21], have shown that the TSI oscillates with a mean value $\overline{W}_\oplus = 1360.8 \pm 0.5\,\mathrm{W/m^2}$ and a peak-to-peak amplitude $\Delta W_\oplus$ equal to about 0.1% its mean value [4]. The TSI is also affected by short-term random variations (superimposed to the 11-year solar cycle), which can reach values of $4.6\,\mathrm{W/m^2}$ within a few days up to weeks [5]. A fluctuation of $W_\oplus$ may also manifest itself on a time scale of minutes, with an amplitude on the order of 0.003% its mean value and peaks of 0.015% during large solar flares [4]. However, TSI fluctuations that occur on time scales smaller than 1 day will be neglected in the succeeding analysis.

The TSI is here assumed to be a Gaussian random variable, whose mean value μ_W is modelled as a sinusoidal fluctuation due to the 11-year solar cycle, as is shown in Fig. 1. In particular, assuming a minimum solar activity at the initial time, the time variation of μ_W is described as

$$\mu_W = W_\oplus^{\min} + \frac{\Delta W_\oplus}{2}\left[1 - \cos\left(\frac{2\,\pi\,t}{\Delta t_c}\right)\right] \tag{3}$$

where $\Delta t_c = 11\,\mathrm{years}$, and $W_\oplus^{\min} \simeq 1360.5\,\mathrm{W/m^2}$ is the TSI at the minimum solar activity, of which the value is chosen such as to fit the available SORCE [21] data in the time interval 2008-2009; see also Fig. 2. The standard deviation σ_W is affected both by a measurement uncertainty in the mean value ($\pm 0.5\,\mathrm{W/m^2}$), and by short-term fluctuations ($\pm 2.3\,\mathrm{W/m^2}$), viz.

$$\sigma_W = \sqrt{0.5^2 + 2.3^2}\,\mathrm{W/m^2} \simeq 2.35\,\mathrm{W/m^2} \tag{4}$$

Using the mathematical model given by Eqs. (3) and (4), it is possible to estimate the effects of the TSI (or SRP) fluctuations on the solar sail optimal transfer trajectory. To that end, the reference optimal transfer trajectory and the corresponding reference optimal control law are first obtained by solving the minimum-time problem (with an indirect approach [22]) assuming a value of TSI equal to $\overline{W}_\oplus$. In other terms, the reference trajectory is designed with a fixed value of SRP calculated at $r = r_\oplus$, equal to $\overline{W}_\oplus/c \simeq 4.54 \times 10^{-6}\,\mathrm{Pa}$.

The flight time is then partitioned into a certain number of arcs of length $\Delta t = 1\,\mathrm{day}$ each. Then, the daily variation of $W_\oplus$ is randomly generated according to the previous Gaussian distribution, and a linear interpolation is used to evaluate the TSI along each arc. At this point, the equations of motion (2) are numerically integrated along each arc using the reference control law. The spacecraft position $\boldsymbol{r}_f = \boldsymbol{r}(t_f)$ and velocity $\boldsymbol{v}_f = \boldsymbol{v}(t_f)$ vectors at the final time t_f are compared to those obtained in the reference trajectory (i.e., $\bar{\boldsymbol{r}}_f$ and $\bar{\boldsymbol{v}}_f$). Finally, the position δ_r and velocity δ_v errors are calculated as

$$\delta_r = \|\boldsymbol{r}_f - \bar{\boldsymbol{r}}_f\| \quad , \quad \delta_v = \|\boldsymbol{v}_f - \bar{\boldsymbol{v}}_f\| \tag{5}$$

The main results of the above procedure are discussed in the next section for different transfer scenarios and solar sail performance, using the Gaussian distribution with a mean value given by Eq. (3) and a standard deviation given by Eq. (4) to estimate the local value of TSI.

Numerical simulations

The effects of TSI fluctuations on the spacecraft transfer trajectory are now studied, as a function of the solar sail performance, for some typical mission scenarios. Three different values of the ratio m/A are considered in the numerical simulations, that is, $m/A = \{8.2,\, 16.5,\, 82.4\}\,\mathrm{g/m^2}$, which are representative of high-, medium- and low-performance sails, respectively. In the reference case, such values of m/A correspond to solar sails with a reference characteristic acceleration

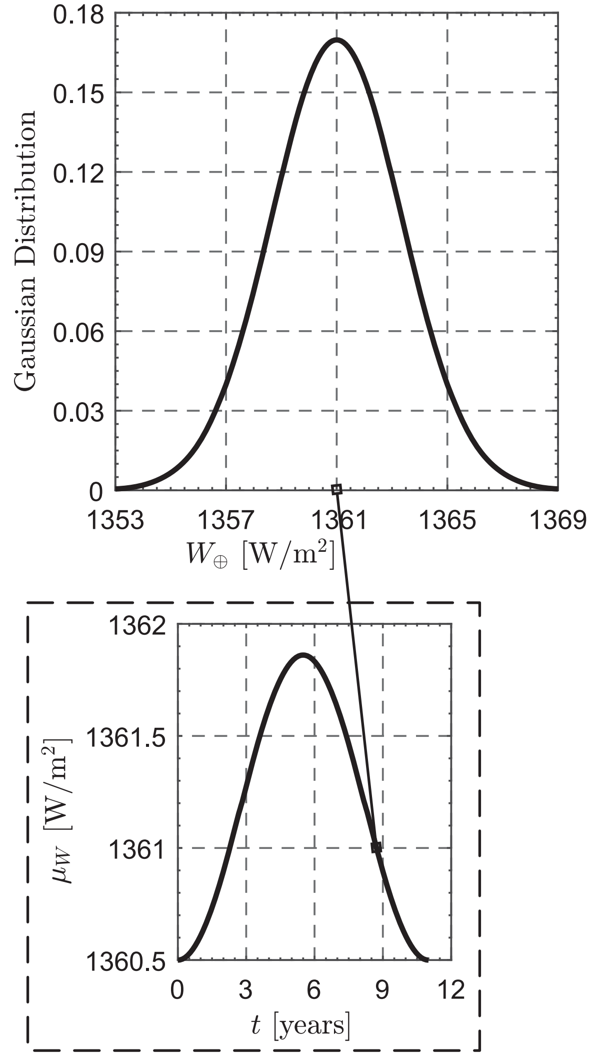

Figure 1 Model of TSI with a Gaussian distribution and a mean value described by a sinusoidal fluctuation due to the 11-year solar cycle.

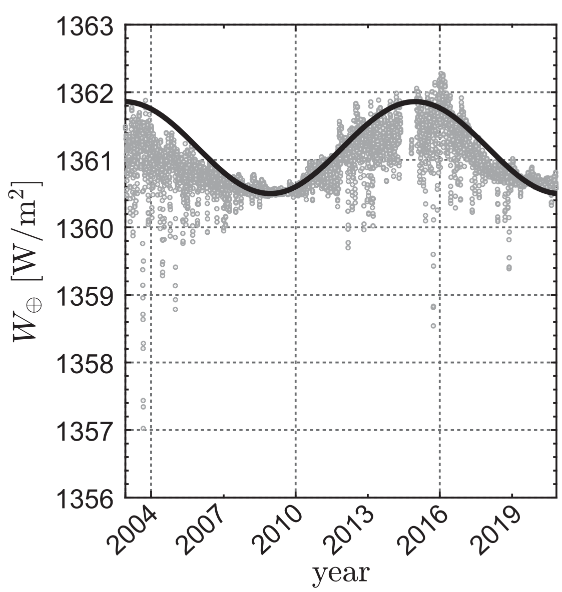

Figure 2 Variation of μ_W due to the 11-year solar cycle modelled as a sinusoidal function and its comparison with real data from SORCE mission.

$a_c = \{0.1,\, 0.5,\, 1\}\,\mathrm{mm/s^2}$, the latter being defined as the maximum magnitude of the sail propulsive acceleration at a distance $r = r_\oplus$ from the Sun, or

$$a_c = \frac{\overline{W}_\oplus\, A}{m\, c}\,(b_1 + b_2 + b_3) \tag{6}$$

Consider a circle-to-circle orbit transfer, in which the parking orbit radius is $r_0 = 1\,\mathrm{au}$ and the target orbit radius is $r_f = \{0.387,\, 0.5,\, 0.723,\, 1.2,\, 1.524\}\,\mathrm{au}$. Note that the cases of $r_f = \{0.387,\, 0.723,\, 1.524\}\,\mathrm{au}$ are representative of a simplified (heliocentric) interplanetary transfer towards {Mercury, Venus, Mars}, when the planet orbital eccentricity and inclination are both neglected. In the reference case, the minimum flight time [23] is reported in Tab. 1.

Table 1 Minimum flight time (days) as a function of r_f and a_c, for a circle-to-circle transfers with $r_0 = 1\,\mathrm{au}$.

	a_c (mm/s^2)		
r_f (au)	0.1	0.5	1
0.387	2536.4	550.0	310.6
0.5	2164.7	463.3	256.4
0.723	1310.1	284.5	217.0
1.2	1104.4	312.9	248.3
1.524	2963.4	653.6	432.5

For each transfer case, that is, for each pair $\{r_f, a_c\}$, 100 numerical simulations have been performed by numerically integrating the equations of motion (2) using a variable-step Adams-Bashforth-Moulton solver scheme [24, 25], with absolute and relative errors of 10^{-12}. The mean and maximum values of $\{\delta_r,\, \delta_v\}$ obtained with Eqs. (5), are reported in Tabs. 2 and 3.

Table 2 Mean/maximum values of δ_r (km) as a function of r_f and a_c, for a circle-to-circle orbit transfers (100 runs).

	a_c (mm/s^2)		
r_f (au)	0.1	0.5	1
0.387	$1.476/1.991 \times 10^6$	$1.890/4.052 \times 10^5$	$1.083/2.296 \times 10^5$
0.5	$5.652/8.460 \times 10^5$	$1.183/2.613 \times 10^5$	$4.710/11.790 \times 10^4$
0.723	$6.030/15.990 \times 10^4$	$2.410/6.270 \times 10^4$	$1.860/5.220 \times 10^4$
1.2	$4.530/8.810 \times 10^4$	$3.830/12.050 \times 10^4$	$3.710/11.680 \times 10^4$
1.524	$4.409/6.776 \times 10^5$	$1.242/2.912 \times 10^5$	$1.220/2.962 \times 10^5$

Table 3 Mean/maximum values of δ_v (m/s) as a function of r_f and a_c, for a circle-to-circle orbit transfers (100 runs).

	a_c (mm/s^2)		
r_f (au)	0.1	0.5	1
0.387	16.5/22.6	11.1/27.0	10.0/26.2
0.5	6.0/9.1	5.3/14.1	5.2/13.5
0.723	0.8/2.1	1.7/3.9	2.5/6.1
1.2	0.3/0.8	1.0/2.8	1.4/3.7
1.524	1.9/2.9	1.5/4.2	2.9/6.3

According to Tabs. 2 and 3, a considerable position error δ_r is obtained when orbit transfers with long flight times are considered. This is due, as expected, to the non-negligible impact of the variation of μ_W related to the 11-year solar cycle. Note that a high value of δ_r is obtained in an orbit lowering (i.e., when $r_f < r_0$), because the propulsive acceleration magnitude undergoes a large deviation from the reference case when the solar sail approaches the Sun. These results are compatible with those obtained by using actual *in-situ* measurements only to model the TSI, but are more conservative. Indeed, the statistical model discussed in this work is based on many years of solar observation, and accounts for a significant stochastic term to model the chaotic and unpredictable TSI fluctuations.

The results obtained in a two-dimensional case are confirmed by a more realistic three-dimensional mission scenario. In this case, the procedure has been applied to a three-dimensional transfer towards Mars and to the near-Earth asteroid 1620 Geographos [26–28], by considering the actual heliocentric orbits of the celestial bodies. The optimal transfer times are shown in Tab. 4 as a function of the sail characteristic acceleration $a_c = \{0.1,\, 0.5,\, 1\}\,\mathrm{mm/s^2}$.

Table 4 Minimum flight time (days) as a function of a_c, for a three-dimensional Earth-Mars and Earth-Geographos transfer.

	a_c (mm/s^2)		
Scenario	0.1	0.5	1
Earth-Mars	3138.0	817.4	381.8
Earth-Geographos	4282.7	806.4	391.7

When the TSI fluctuations are taken into account, the errors δ_r and δ_v obtained through 100 runs are shown in Fig. 3, whereas their mean and maximum values are summarized in Tabs. 5 and 6.

Table 5 Mean/maximum values of δ_r (km) as a function of a_c, for an Earth-Mars and an Earth-Geographos transfer (100 runs).

	$\bar{a}_c$ (mm/s^2)		
Scenario	0.1	0.5	1
Earth-Mars	555 300/742 800	125 600/335 700	97 000/230 000
Earth-Geographos	797 500/1 126 600	37 600/93 300	27 600/76 000

Table 6 Mean/maximum values of δ_v (m/s) as a function of a_c, for an Earth-Mars and an Earth-Geographos transfer (100 runs).

	$\bar{a}_c$ (mm/s^2)		
Scenario	0.1	0.5	1
Earth-Mars	3.2/4.6	2.5/5.6	2.0/4.9
Earth-Geographos	99.3/139.8	5.2/13.6	2.6/5.9

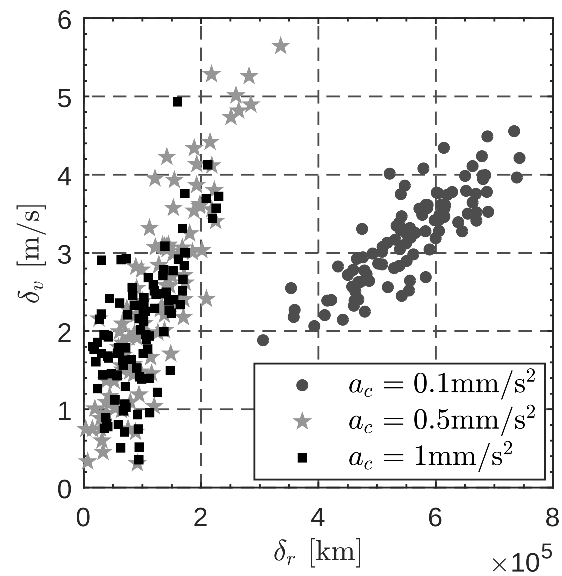

a) Earth-Mars transfer.

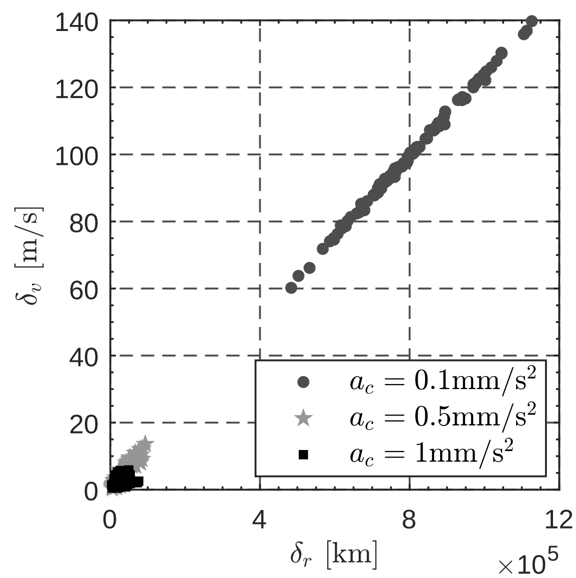

b) Earth-Geographos transfer.

Figure 3 Values of errors $\{\delta_r, \delta_v\}$ in a three-dimensional orbit transfer (100 runs).

Conclusions

This Note has analyzed the effects of fluctuations of the total solar irradiance (equivalently, the fluctuations of the solar radiation pressure) on optimal solar sail heliocentric transfers. Both two-dimensional circle-to-circle and more realistic three-dimensional transfer scenarios have been investigated, by considering a low-, medium-, and high-performance solar sail. A procedure has been proposed to evaluate the deviation of the solar sail spacecraft from its reference trajectory (i.e., the trajectory obtained without any solar irradiance fluctuation) when the total solar irradiance is modelled as a random variable with a Gaussian distribution.

The numerical simulations have shown that this deviation is small for a high-performance sail. However, in the case of transfers requiring long flight times, the final error in position and velocity is well outside the typical mission requirements for targeting accuracy. A natural extension of this work is therefore to introduce a suitable control law that is able to counteract the irradiance fluctuations and to allow the spacecraft to reach the desired target state. Such a control system could exploit the properties of electrochromic materials to adjust the propulsive acceleration magnitude and direction, in response to environmental fluctuations.

Acknowledgements

This work is supported by the University of Pisa, Progetti di Ricerca di Ateneo (Grant no. PRA 2018 44).

References

[1] Wright, J. L., *Space Sailing*, Gordon and Breach Science Publishers, 1992, pp. 223–233, ISBN: 978-2881248429.

[2] McInnes, C. R., *Solar Sailing: Technology, Dynamics and Mission Applications*, chap. 2, Springer-Verlag Berlin, 1999, pp. 32–55, ISBN: 978-1-85233-102-3.

[3] Pap, J. M. and Fröhlich, C., "Total solar irradiance variations," *Journal of Atmospheric and Solar-Terrestrial Physics*, Vol. 61, No. 1-2, Jan. 1999, pp. 15–24. doi: https://doi.org.10.1016/S1364-6826(98)00112-6.

[4] Fröhlich, C. and Lean, J., "Solar radiative output and its variability: Evidence and mechanisms," *Astronomy and Astrophysics Review*, Vol. 12, No. 4, 2004, pp. 273–320. doi: https://doi.org.10.1007/s00159-004-0024-1.

[5] Kopp, G. and Lean, J. L., "A new, lower value of total solar irradiance: Evidence and climate significance," *Geophysical Research Letters*, Vol. 38, No. 1, Jan. 2011, pp. 1–7. doi: https://doi.org.10.1029/2010GL045777.

[6] Fox, P., *Solar Activity and Irradiance Variations*, American Geophysical Union (AGU), 2013, pp. 141–170, ISBN: 9781118665909.

[7] Vulpetti, G., "Effect of the total solar irradiance variations on solar-sail low-eccentricity orbits," *Acta Astronautica*, Vol. 67, No. 1-2, July 2010, pp. 279–283. doi: https://doi.org.10.1016/j.actaastro.2010.02.004.

[8] Vulpetti, G., "Total solar irradiance fluctuation effects on sailcraft-Mars rendezvous," *Acta Astronautica*, Vol. 68, No. 5-6, March 2011, pp. 644–650. doi: https://doi.org.10.1016/j.actaastro.2010.01.010.

[9] Niccolai, L., Anderlini, A., Mengali, G., and Quarta, A. A., "Impact of solar wind fluctuations on Electric Sail mission design," *Aerospace Science and Technology*, Vol. 82-83, Nov. 2018, pp. 38–45. doi: https://doi.org.10.1016/j.ast.2018.08.032.

[10] Niccolai, L., Anderlini, A., Mengali, G., and Quarta, A. A., "Electric sail displaced orbit control with solar wind uncertainties," *Acta Astronautica*, Vol. 162, September 2019, pp. 563–573. doi: https://doi.org.10.1016/j.actaastro.2019.06.037.

[11] Caruso, A., Niccolai, L., Mengali, G., and Quarta, A. A., "Electric sail trajectory correction in presence of environmental uncertainties," *Aerospace Science and Technology*, Vol. 94, Nov. 2019. doi: https://doi.org.10.1016/j.ast.2019.105395.

[12] Janhunen, P., "Electric Sail for Spacecraft Propulsion," *Journal of Propulsion and Power*, Vol. 20, No. 4, July 2004, pp. 763–764. doi: https://doi.org.10.2514/1.8580.

[13] Mengali, G. and Quarta, A. A., "Optimal three-dimensional interplanetary rendezvous using nonideal solar sail," *Journal of Guidance, Control, and Dynamics*, Vol. 28, No. 1, January-February 2005, pp. 173–177. doi: https://doi.org.10.2514/1.8325.

[14] Dachwald, B., Macdonald, M., McInnes, C. R., Mengali, G., and Quarta, A. A., "Impact of optical degradation on solar sail mission performance," *Journal of Spacecraft and Rockets*, Vol. 44, No. 4, July-August 2007, pp. 740–749. doi: https://doi.org.10.2514/1.21432.

[15] McInnes, C. R., "Approximate Closed-Form Solution for Solar Sail Spiral Trajectories with Sail Degradation," *Journal of Guidance, Control, and Dynamics*, Vol. 37, No. 6, 2014, pp. 2053–2057. doi: https://doi.org.10.2514/1.G000225.

[16] Chujo, T., Ishida, H., Mori, O., and Kawaguchi, J., "Liquid Crystal Device with Reflective Microstructure for Attitude Control," *Journal of Spacecraft and Rockets*, Vol. 55, No. 6, 2018, pp. 1509–1518. doi: https://doi.org.10.2514/1.A34165.

[17] Hu, T., Gong, S., Mu, J., Li, J., Wang, T., and Qian, W., "Switch programming of reflectivity control devices for the coupled dynamics of a solar sail," *Advances in Space Research*, Vol. 57, No. 5, March 2016, pp. 1147–1158. doi: https://doi.org.10.1016/j.asr.2015.12.029.

[18] Wie, B., "Thrust Vector Control Analysis and Design for Solar-Sail Spacecraft," *Journal of Spacecraft and Rockets*, Vol. 44, No. 3, 2007, pp. 545–557. doi: https://doi.org.10.2514/1.23084.

[19] Sauer, C. G., "Optimum solar-sail interplanetary trajectories," *AIAA/AAS Astrodynamics Conference*, San Diego (CA), Aug. 1976.

[20] Niccolai, L., Quarta, A. A., and Mengali, G., "Analytical Solution of the Optimal Steering Law for Non-Ideal Solar Sail," *Aerospace Science and Technology*, Vol. 62, March 2017, pp. 11–18. doi: https://doi.org.10.1016/j.ast.2016.11.031.

[21] Mauceri, S., Pilewskie, P., Richard, E., Coddington, O., Harder, J., and Woods, T., "Revision of the Sun's Spectral Irradiance as Measured by SORCE SIM," *Solar Physics*, Vol. 293, No. 12, 2018. doi: https://doi.org.10.1007/s11207-018-1379-1.

[22] Bryson, A. E. and Ho, Y. C., *Applied Optimal Control*, chap. 2, Hemisphere Publishing Corporation, New York, NY, 1975, pp. 71–89, ISBN: 0-891-16228-3.

[23] Caruso, A., Quarta, A. A., and Mengali, G., "Comparison between direct and indirect approach to solar sail circle-to-circle orbit raising optimization," *Astrodynamics*, Vol. 3, No. 3, Sept. 2019, pp. 273–284. doi: https://doi.org.10.1007/s42064-019-0040-x.

[24] Shampine, L. F. and Gordon, M. K., *Computer Solution of Ordinary Differential Equations: The Initial Value Problem*, chap. 10, W. H. Freeman, San Francisco, 1975, ISBN: 978-0716704614.

[25] Shampine, L. F. and Reichelt, M. W., "The MATLAB ODE Suite," *SIAM Journal on Scientific Computing*, Vol. 18, No. 1, January 1997, pp. 1–22. doi: https://doi.org.10.1137/S1064827594276424.

[26] Ryabova, G. O., "Asteroid 1620 Geographos: I. Rotation," *Solar System Research*, Vol. 36, No. 2, 2002, pp. 168–174. doi: https://doi.org.10.1023/A:1015226417427.

[27] Ryabova, G. O., "Asteroid 1620 Geographos: II. Associated meteor streams," *Solar System Research*, Vol. 36, No. 3, 2002, pp. 234–247. doi: https://doi.org.10.1023/A:1015897215612.

[28] Ryabova, G. O., "Asteroid 1620 Geographos: III. Inelastic relaxation in the vicinity of the poles," *Solar System Research*, Vol. 38, No. 3, 2004, pp. 212–218. doi: https://doi.org.10.1023/B:SOLS.0000030861.89529.18.